AJNR

Temporal Characteristics of CSF-Venous Fistulas on Digital Subtraction Myelography

I. Mark, A. Madhavan, M. Oien, J. Verdoorn, J. Benson, J. Cutsforth-Gregory, W. Brinjikji and P. Morris

Temporal Characteristics of CSF-Venous Fistulas on Digital Subtraction Myelography

I. Mark, A. Madhavan, M. Oien, J. Verdoorn, J. Benson, J. Cutsforth-Gregory, W. Brinjikji, and P. Morris

ABSTRACT

BACKGROUND AND PURPOSE: CSF-venous fistula can be diagnosed with multiple myelographic techniques; however, no prior work has characterized the time to contrast opacification and the duration of visualization. The purpose of our study was to evaluate the temporal characteristics of CSF-venous fistula on digital subtraction myelography.

MATERIALS AND METHODS: We reviewed the digital subtraction myelography images of 26 patients with CSF-venous fistulas. We evaluated how long the CSF-venous fistula took to opacify after contrast reached the spinal level of interest and how long it remained opacified. Patient demographics, CSF-venous fistula treatment, brain MR imaging findings, CSF-venous fistula spinal level, and CSF-venous fistula laterality were recorded.

RESULTS: Eight of the 26 CSF-venous fistulas were seen on both the upper- and lower-FOV digital subtraction myelography, for a total of 34 CSF-venous fistula views evaluated on digital subtraction myelography. The mean time to appearance was 9.1 seconds (range, 0–30 seconds). Twenty-two (84.6%) of the CSF-venous fistulas were on the right. The highest fistula level was C7, while the lowest was T13 (13 rib-bearing vertebral bodies). The most common CSF-venous fistula levels were T6 (4 patients) followed by T8, T10, and T11 (3 patients each). The mean age was 58.3 years (range, 31.7–87.6 years). Sixteen patients were women (61.5%).

CONCLUSIONS: This is the first study to report the temporal characteristics of CSF-venous fistulas using digital subtraction myelography. We found that on average, the CSF-venous fistula appeared 9.1 seconds (range, 0–30 seconds) after intrathecal contrast reached the spinal level.

ABBREVIATIONS: CTM = CT myelography; CVF = CSF-venous fistula; DSM = digital subtraction myelography; SIH = spontaneous intracranial hypotension

Spontaneous intracranial hypotension (SIH), a misnomer better characterized as low CSF volume from a spinal cause, can be a debilitating disease and commonly presents with orthostatic headache.[1] Spontaneous spinal CSF leaks can be classified as ventral dural tears (type 1a), posterolateral CSF leaks (type 1b), ruptured meningeal diverticular (type 2), or CSF-venous fistula (CVF) (type 3).[2] CVFs are challenging to diagnose because they are occult on spine MR imaging and are rarely seen on conventional CT myelography (CTM). Thus, myelographic techniques with high spatial and temporal resolution are necessary. Myelography technique varies widely but most commonly includes dynamic CTM[3] or digital subtraction myelography (DSM),[4,5] both of which acquire images immediately after the injection of intrathecal contrast and both of which are performed with the patient in the lateral decubitus position when assessing a CVF. The timing of when CVFs are first visible on myelography and for how long they remain opacified has not been studied. The purpose of this article was to evaluate CVF temporal characteristics on DSM.

MATERIALS AND METHODS

We retrospectively reviewed an internal database following institutional review board clearance for patients with DSM-proved CVF from January to September 2022 at a single institution. All DSMs were performed by neuroradiologists in our spine practice who specialize in SIH and CVF evaluation. All images were reviewed for CVF temporal characteristics by a single neuroradiologist in our spine practice (I.M.). DSM images were reviewed for CVF laterality and spinal level. The time to appearance was measured as the time from when intrathecal contrast reached the CVF spinal level to when the CVF was first seen. The duration of time that the fistula was visible was also determined. All DSM images were reviewed, including the upper run focusing on the thoracic spine and the lower run focusing on the thoracolumbar

Individual CVF information that includes the laterality, spinal level, and temporal characteristics

Side	Level	Upper: Time to Appear/Duration (sec)	Lower: Time to Appear/Duration (sec)
R	C7	12/37+	−
R	T1	10/46+	−
R	T2	3/27+	−
L	T2	12/28+	−
R	T3	3/59+	−
R	T4	1/54	−
R	T4	6/72+	N
R	T5	2/51+	N
R	T5	5/52	−
L	T6	5/41	−
L	T6	7/67+	−
R	T6	11/68	7/67
R	T6	24/35	7/45
L	T7	3/60	0/58
R	T7	16/24	10/38
R	T8	4/51+	−
R	T8	6/49+	11/36+
R	T8	18/38+	N
R	T9	12/54+	14/50+
R	T10	15/54+	N
R	T10	−	5/44+
R	T10	30/34	14/36
R	T11	4/50	3/49+
R	T11	−	14/38+
R	T11	22/73+	N
R	T13	−	6/42+

Note:—The en dash indicates not in the FOV; N, not seen but in the FOV; +, the CVF is opacified on the last image; R, right; L, left.

spine. When the CVF was seen in both the upper and lower DSM images on the same patient, the temporal characteristics were averaged. In cases in which the CVF was no longer visualized before the last image, we also noted whether intrathecal contrast remained at that spinal level.

Additional patient information such as sex, age, and treatment were recorded. Pre-DSM brain MR imaging was evaluated by a neuroradiologist (A.M.) for signs of SIH using a previously described quantitative scale (Bern score).[6]

DSM Technique

All DSMs were performed with the patient under moderate sedation in the lateral decubitus position on a tiltable table with or without a wedge to elevate the patient's hips to achieve approximately 4°–8° of spinal tilt.[7] Imaging was performed at a rate of 1 frame/second. The thecal sac was accessed at L2–L3 or below with a 20- or 22-ga needle, with the intrathecal needle position confirmed by 0.5 mL of iohexol (Omnipaque 300; GE Healthcare). Approximately 5–10 mL of normal saline was slowly infused into the thecal sac for pressurization followed by a hand injection of 6 mL of Omnipaque, while imaging from the cervicothoracic junction to the lower thoracic spine; the caudal FOV depended on the patient's body habitus. We used 5–10 mL of normal saline to flush the line. Then, a second bolus of 5 mL of contrast was injected while imaging from the needle access site and extending cranially, normally extending to the mid-thoracic spine. The connecting tube and needle were cleared with sterile saline, but we did not routinely pressurize the thecal sac with saline after this contrast injection. The duration of image acquisition was determined by

the individual proceduralist. This variability was 1 factor that led to our desire to study CVF temporal characteristics.

RESULTS

Patient Demographics and Brain MR Imaging Findings

Twenty-six patients with CVF on DSM were included in this study. The mean age was 58.3 years (range, 31.7–87.6 years). Sixteen patients were women (61.5%). The mean Bern score was 4.2 (SD, 2.6) (range, 0–8). The occurrence of SIH findings was as follows: suprasellar cistern effacement of ≤4 mm (61.5%), pachymeningeal enhancement (57.7%), venous sinus engorgement (15.4%), subdural fluid collection (7.7%), prepontine cistern effacement of ≤5 mm (80.8%), and mamillopontine distance of ≤6.5 mm (80.8%). None of the patients had been treated with transvenous catheter embolization, epidural blood patch, fibrin glue injection, or surgical ligation before DSM. All patients underwent transvenous catheter embolization with Onyx (Medtronic) for treatment after DSM.

CVF Level and Laterality

The highest fistula level was C7, while the lowest was T13 (13 rib-bearing vertebral bodies). The most common CVF levels were T6 (4 patients) followed by T8, T10, and T11 (3 patients each). Twenty-two (84.6%) CVFs were on the right side. Patient-specific details are listed in the Table.

### CVF Temporal Characteristics

Of the 26 patients, 8 had CVFs that were seen on the upper and lower runs. The mean time from contrast reaching the spinal level to the time of CVF appearance was 9.1 seconds (range, 0–30 seconds). The mean duration of CVF opacification was 48.1 seconds (range, 24–73 seconds). An imaging example of the CVF temporal characteristics on DSM is shown in the Figure. Of the 34 CVFs, 18 CVFs remained opacified on the last DSM image acquired, so we could not assess further duration of contrast opacification beyond the final acquired image. Sixteen CVFs disappeared before the last DSM image, with a mean CVF duration of 49.8 seconds (range, 24–68 seconds). Of the 16 CVFs that disappeared before the last image, 14 (87.5%) had intrathecal contrast at the CVF level (6 of which were faint) and 2 (12.5%) no longer had intrathecal contrast at the CVF level.

CVF Temporal Characteristics by Location

Thirteen CVFs were in the cervical or upper thoracic spine (C7–T6), with a mean time to appearance of 7.0 seconds (range, 1–15.5 seconds), a mean duration of contrast opacification of 49.3 seconds (range, 27–72 seconds), and a mean combined time of 56.3 seconds. The 13 CVFs in the lower thoracic spine (T7–T13) had a similar mean combined time of 58.0 seconds, but a slightly longer mean time to appearance (11.2 seconds) and a shorter mean duration (46.8 seconds).

DSM Upper-versus-Lower Runs

The spinal level of the CVF was within the FOV in both the upper and lower runs in 13 patients. All were seen on the upper run, compared with only 8 (61.5%) on the lower run. All cases
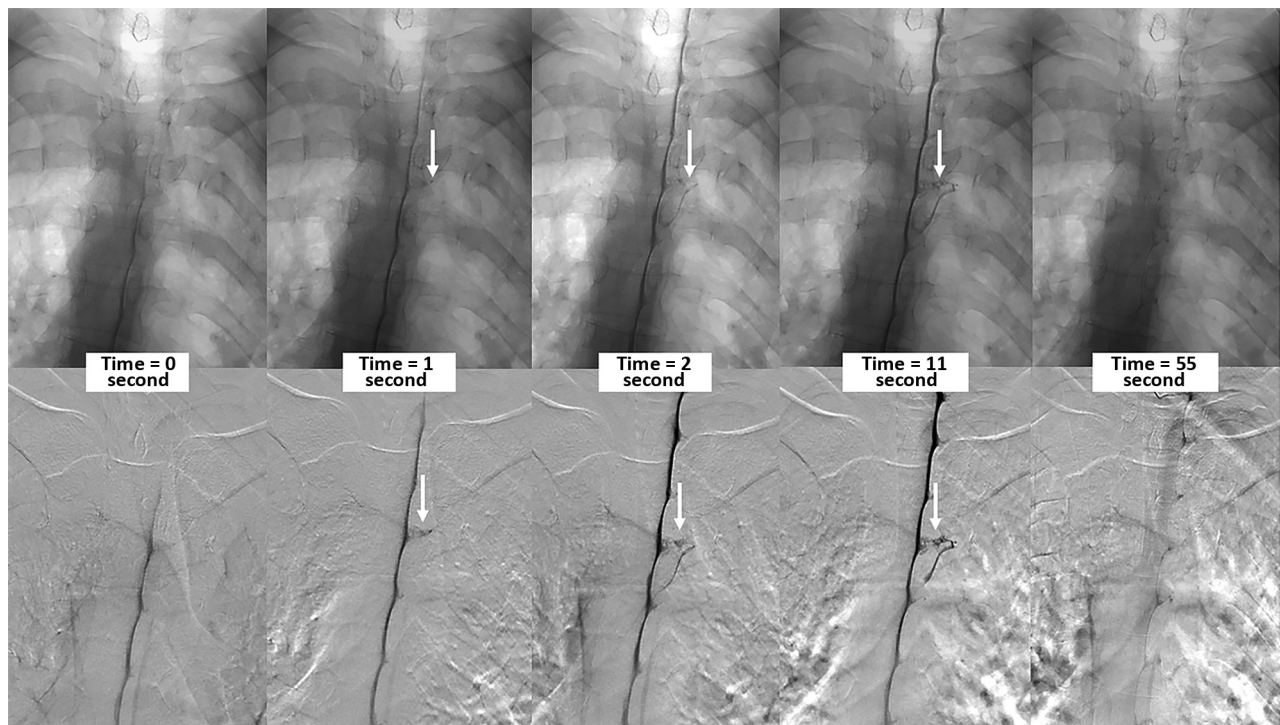
FIGURE. Multiple imaging timepoints of a right (DSM laterality is opposite conventional radiographs) T4 CVF (*arrows*) in a single patient. The *upper row* shows nonsubtracted fluoroscopy images, and the *lower row* shows DSM images. At time = 0, the contrast column reaches the level of the CVF. One second after, intrathecal contrast starts to fill the CVF, which is better seen at the 2- and 11-second images. The CVF is no longer visible 54 seconds after the initial appearance.

followed our standard technique, with the upper run acquired before the lower run.

DISCUSSION

In the current study, we evaluated the temporal characteristics of CVF on DSM. We found that CVFs take 9.1 seconds to appear once contrast reaches the spinal level of the CVF and remain visible for an additional 48.1 seconds. Because CVFs are challenging to diagnose, multiple modalities (DSM, CTM, MR myelography) and image-acquisition timing (dynamic-versus-nondynamic) have been used. The variety of myelographic techniques is due, in part, to resource availability as well as lack of understanding of how and when CVFs opacify with contrast. This is the first study to evaluate CVF temporal characteristics and could help to improve future myelographic techniques in the evaluation of CVF.

CVFs were first described with DSM.[8] Since that discovery, multiple modalities have been used for CVF diagnosis.[7,9,10] DSM has the advantage of higher temporal resolution because our technique acquires images at a rate of 1 frame per second. One challenge with DSM lies in the uncertainty of knowing how long to image. The dilemma of when to image and for how long could also apply to CTM. Prior work describing ultrafast dynamic CTM reported approximately 15 seconds per acquisition of the cervical and thoracic spine.[11] The acquisition time would be longer when including the lumbar spine.

Depending on the table tilt, spine curvature, and CSF dynamics, our practice observes intrathecal contrast flowing at various rates during DSM. Therefore, we measured the time of CVF appearance from when the contrast reached the spinal level. We found that on average, CVFs opacify with contrast 9.1 seconds after intrathecal contrast reaches the CVF level. Twelve of 33 (36.4%) CVFs opacified within the first 5 seconds, while 5 (18.2%) took at least 15 seconds to appear. On average, the CVF remained opacified for 48.1 seconds. Only 3 (9.1%) CVFs disappeared before 30 seconds, while 18 (52.9%) remained opacified on the final image. If the spine were imaged 30 seconds after the contrast reached a particular spinal level, all cases of CVF from our cohort would be seen on at least 1 frame.

Prior work has suggested that respiratory techniques during myelography could help opacify the CVF. Amrhein et al[12] described increased conspicuity of the CVF at end-inspiration. Other work has shown that the CSF-to-venous pressure gradient can be increased with resisted inspiration.[13] It is unknown how resisted inspiration would affect the temporal characteristics of CVF, but it could conceivably decrease the time to appearance and duration. The duration of CVF opacification should depend, in part, on the venous outflow, with most CVFs draining into the azygos system and, in turn, into the superior vena cava (SVC). Prior work has shown that the SVC-azygos junction can have efferent flow depending on the cardiac cycle,[14] which could further delay emptying of the azygos system. The effect of general anesthesia and positive pressure ventilation are unknown, but increased intrathoracic pressure could pressurize the azygos system and contribute to delayed opacification and emptying of the CVF. While general anesthesia would optimize motion control, we did not find that motion obscured CVF visualization in our cases.

Thirteen of our patients had CVFs at a spinal level that was within the FOV on both the upper and lower runs of the DSM. The CVF was visualized on the upper run in all cases. Most interesting, only 61.5% of CVFs were also seen on the lower run, despite being within the FOV. In each of these cases, the upper run was acquired first, and the lower run, second. This result could be attributed to the use of a postcontrast saline chaser for the upper run but not the lower run. Work by Caton et al[15] suggests that a CVF may need a certain pressure to open; likewise, there may be a subsequent pressure drop. With our technique, the contrast from the lower run and the lack of a saline chaser may not provide the necessary pressure to open the CVF seen on the upper run. The ideal saline chaser size and rate of infusion are not known, but theoretically, a more robust chaser could make the CVF appear sooner. Further study comparing the DSM yield with and without positive pressurization of the thecal sac could better elucidate these observations.

Our study has limitations. Our sample size is small, just 26 patients, yet this represents one of the largest studies on CVF using DSM. A larger sample size may help to categorize the temporal characteristics by spinal level. Second, the CVF was opacified on the last image in more than one-half of our patients; therefore, we do not know the true duration of opacification. This limitation falsely decreases the calculated duration of opacification. Also, we imaged patients for only a short duration after the injection of contrast. Prior work has used a delayed image acquisition with conventional nondynamic CTM[16] and MR myelography[17,18] to evaluate CVFs. Therefore, it would be difficult to apply our findings to those cases of delayed imaging. Additionally, dynamic myelography technique can differ at each institution (modality, saline chaser, contrast amount, breathing instructions) and, therefore, limits the generalization of these results. Finally, we were unable to detail the time between the injection of contrast and the time of first image acquisition. While our typical procedure has a 5- to 7-second delay, this is variable and it cannot be measured retrospectively.

CONCLUSIONS

This is the first study to report on the temporal characteristics of CVF using DSM. We found that on average, the CVF appeared 9.1 seconds after the intrathecal contrast reached the CVF spinal level.

Disclosure forms provided by the authors are available with the full text and PDF of this article at www.ajnr.org.

REFERENCES

1. Kranz PG, Gray L, Malinzak MD, et al. **Spontaneous intracranial hypotension: pathogenesis, diagnosis, and treatment.** *Neuroimaging Clin N Am* 2019;29:581–94 CrossRef Medline
2. Schievink WI, Maya MM, Jean-Pierre S, et al. **A classification system of spontaneous spinal CSF leaks.** *Neurology* 2016;87:673–79 CrossRef Medline
3. Luetmer PH, Mokri B. **Dynamic CT myelography: a technique for localizing high-flow spinal cerebrospinal fluid leaks.** *AJNR Am J Neuroradiol* 2003;24:1711–14 Medline
4. Schievink WI, Moser FG, Maya MM, et al. **Digital subtraction myelography for the identification of spontaneous spinal CSF-venous fistulas.** *J Neurosurg Spine* 2016;24:960–64 CrossRef Medline
5. Schievink WI, Maya MM, Moser FG, et al. **Lateral decubitus digital subtraction myelography to identify spinal CSF-venous fistulas in spontaneous intracranial hypotension.** *J Neurosurg Spine* 2019 Sep 13. [Epub ahead of print] CrossRef Medline
6. Dobrocky T, Grunder L, Breiding PS, et al. **Assessing spinal cerebrospinal fluid leaks in spontaneous intracranial hypotension with a scoring system based on brain magnetic resonance imaging findings.** *JAMA Neurol* 2019;76:580–87 CrossRef Medline
7. Kim DK, Brinjikji W, Morris PP, et al. **Lateral decubitus digital subtraction myelography: tips, tricks, and pitfalls.** *AJNR Am J Neuroradiol* 2020;41:21–28 CrossRef Medline
8. Schievink WI, Moser FG, Maya MM. **CSF-venous fistula in spontaneous intracranial hypotension.** *Neurology* 2014;83:472–73 CrossRef Medline
9. Callen AL, Timpone VM, Schwertner A, et al. **Algorithmic multimodality approach to diagnosis and treatment of spinal CSF leak and venous fistula in patients with spontaneous intracranial hypotension.** *AJR Am J Roentgenol* 2022;219:292–301 CrossRef Medline
10. Mamlouk MD, Ochi RP, Jun P, et al. **Decubitus CT myelography for CSF-venous fistulas: a procedural approach.** *AJNR Am J Neuroradiol* 2021;42:32–36 CrossRef Medline
11. Thielen KR, Sillery JC, Morris JM, et al. **Ultrafast dynamic computed tomography myelography for the precise identification of high-flow cerebrospinal fluid leaks caused by spiculated spinal osteophytes.** *J Neurosurg Spine* 2015;22:324–31 CrossRef Medline
12. Amrhein TJ, Gray L, Malinzak MD, et al. **Respiratory phase affects the conspicuity of CSF-venous fistulas in spontaneous intracranial hypotension.** *AJNR Am J Neuroradiol* 2020;41:1754–56 CrossRef Medline
13. Mark IT, Amans MR, Shah VN, et al. **Resisted inspiration: a new technique to aid in the detection of CSF-venous fistulas.** *AJNR Am J Neuroradiol* 2022;43:1544–47 CrossRef Medline
14. Morita S, Suzuki K, Masukawa A, et al. **Identification of efferent flow in the superior vena cava and azygos vein confluence using cine phase-contrast MRI: speculation of the role of the azygos arch valves.** *Magn Reson Imaging* 2010;28:1306–10 CrossRef Medline
15. Caton MT Jr, Laguna B, Soderlund KA, et al. **Spinal compliance curves: preliminary experience with a new tool for evaluating suspected CSF venous fistulas on CT myelography in patients with spontaneous intracranial hypotension.** *AJNR Am J Neuroradiol* 2021;42:986–92 CrossRef Medline
16. Clark MS, Diehn FE, Verdoorn JT, et al. **Prevalence of hyperdense paraspinal vein sign in patients with spontaneous intracranial hypotension without dural CSF leak on standard CT myelography.** *Diagn Interv Radiol* 2018;24:54–59 CrossRef Medline
17. Chazen JL, Robbins MS, Strauss SB, et al. **MR myelography for the detection of CSF-venous fistulas.** *AJNR Am J Neuroradiol* 2020;41:938–40 CrossRef Medline
18. Madhavan AA, Carr CM, Benson JC, et al. **Diagnostic yield of intrathecal gadolinium MR myelography for CSF leak localization.** *Clin Neuroradiol* 2022;32:537–45 CrossRef Medline